Dinuclear Manganese(II) Complexes with the $\{Mn_2(\mu\text{-carboxylato})_2\}^{2+}$ Core and Their Transformation to (μ-Oxo)bis(μ-carboxylato)dimanganese(III) Complexes

Tomoaki Tanase[†] and Stephen J. Lippard*

Department of Chemistry, Massachusetts Institute of Technology, Cambridge, Massachusetts 02139

Received February 24, 1995[⊗]

Dinuclear Mn(II) complexes having a substitutionally labile $\{Mn_2(\mu\text{-carboxylato})_2\}^{2+}$ core were readily synthesized by using the dinucleating ligand XDK, where H_2XDK = *m*-xylenediamine bis(Kemp's triacid imide). Reaction of $Mn(NO_3)_2{\cdot}6H_2O$ with $Na_2XDK{\cdot}4H_2O$ resulted in quantitative formation of $[Mn_2(XDK)(NO_3)(CH_3OH)_4(H_2O)_2](NO_3)$ (**1**), which was characterized by X-ray crystallography (monoclinic, $P2_1/c$, a = 11.226(1) Å, b = 13.120(1) Å, c = 30.467(3) Å, β = 98.739(8)°, V = 4435.2(7) Å^3, Z = 4, and R = 0.034 and R_w = 0.045 for 4957 independent reflections with $I > 3\sigma(I)$). The cation in **1** contains two octahedral Mn(II) ions bridged by the two carboxylate groups of XDK (Mn···Mn = 4.8497(7) Å), the terminal positions being occupied by labile solvent molecules and a nitrate anion. Compound **1** proved to be a good precursor for preparing a series of bis(μ-carboxylato)dimanganese(II) complexes with N-donor bidentate terminal ligands. Reaction of **1** with 2,2′-dipyridyl (bpy), 4,4′-dimethyl-2,2′-dipyridyl (4,4′-Me_2bpy), or 1,10-phenanthroline (phen) afforded $[Mn_2(XDK)L_2(NO_3)_2(H_2O)]$ (L = bpy (**2**), 4,4′-Me_2bpy (**3**), or phen (**4**)) in high yields. The structure of **2**·CH_2Cl_2 was shown by X-ray crystallography to have an asymmetric dinuclear Mn(II) core bridged by XDK with a Mn···Mn distance of 4.557(2) Å. One Mn(II) atom adopts an octahedral geometry while the other has a distorted trigonal bipyramidal environment (monoclinic, $P2_1/c$, a = 14.491(2) Å, b = 17.954(2) Å, c = 22.492(3) Å, β = 108.787(9)°, V = 5537(1) Å^3, Z = 4, and R = 0.055 and R_w = 0.058 for 4438 independent reflections with $I > 3\sigma(I)$). Compounds **2** and **3** are readily oxidized by excess *tert*-butyl hydroperoxide in methanol to afford (μ-oxo)bis(μ-carboxylato)dimanganese(III) complexes, $[Mn_2(\mu\text{-O})(XDK)L_2(NO_3)_2]$ (L = bpy (**5**) and 4,4′-Me_2bpy (**6**)). The crystal structure of **6**·2.5CH_3OH revealed two octahedral Mn(III) ions symmetrically bridged by two carboxylate groups of XDK and an oxo ligand. The metal−metal separation is 3.170(2) Å, and the two 4,4′-Me_2bpy ligands lie in anti arrangement with respect to the Mn−O−Mn plane (orthorhombic, *Pbcn*, a = 41.636(9) Å, b = 13.108(1) Å, c = 22.422(9) Å, V = 12237(2) Å^3, Z = 8, and R = 0.073 and R_w = 0.085 for 3731 independent reflections with $I > 3\sigma(I)$). Complexes **5** and **6** could be prepared in low yields by air oxidation of **2** and **3**, respectively, a reaction that was readily reversed by treatment with hydrogen peroxide. Reaction of **2**−**4** with an excess amount of hydrogen peroxide quite slowly evolved dioxygen, whereas the solvento dimanganese(II) compound **1** efficiently disproportionated hydrogen peroxide by first converting to a heterogeneous catalyst. A mononuclear complex, $[Mn(HXDK)_2(H_2O)_2]$ (**7**), prepared independently, and MnO_2 were isolated from the heterogeneous mixture, and the latter was shown to be the active species for disproportionating hydrogen peroxide.

Introduction

Multinuclear manganese complexes are of considerable current interest as synthetic models for the active sites of manganese-containing metalloenzymes such as the oxygen-evolving center (OEC) of photosystem II (PSII), manganese catalase and pseudocatalase, and manganese ribonucleotide reductase (RR).[1] Recently, a tetranuclear structural model for the OEC in PSII has been proposed on the basis of EXAFS and XANES studies, involving two bis(μ-oxo)dimanganese units (Mn···Mn = 2.7 Å) linked by (μ-oxo)bis(μ-carboxylato) bridges (Mn···Mn = 3.3 Å).[1,2] Carboxylate-bridged dinuclear manganese centers that catalyze the disproportionation of hydrogen peroxide also appear to exist in the active sites of pseudocatalase from *Lactobacillus plantarum*[3] and catalase from *Thermus thermophilus*.[4] A low-resolution X-ray crystallographic analysis of the latter enzyme demonstrated that two manganese ions are located at a distance of ~3.6 Å,[4a] and an EPR study indicated that the dinuclear core can exist in three oxidation states, $Mn^{II}Mn^{II}$, $Mn^{II}Mn^{III}$, and $Mn^{III}Mn^{IV}$.[4b] From spectroscopic studies, a mechanism involving oscillation between the $Mn^{II}Mn^{II}/Mn^{III}Mn^{III}$ oxidation states has been proposed for the dimanganese catalase reaction,[1,3−5] and functional model systems having (μ-alkoxo)(μ-carboxylato)dimanganese(II)[6] and bis(μ-alkoxo)di-

[†] Permanent address: Department of Chemistry, Faculty of Science, Toho University, Miyama 2-2-1, Funabashi, Chiba 274, Japan.

[⊗] Abstract published in *Advance ACS Abstracts,* July 15, 1995.

(1) (a) Wieghardt, K. *Angew. Chem., Int. Ed. Engl.* **1989**, *28*, 1153. (b) Wieghardt, K. *Angew. Chem., Int. Ed. Engl.* **1994**, *33*, 725. (c) Christou, G. *Acc. Chem. Res.* **1989**, *22*, 328. (d) Vincent, J. B.; Christou, G. *Adv. Inorg. Chem.* **1989**, *33*, 197. (e) Que, L., Jr.; True, A. E. *Prog. Inorg. Chem.* **1990**, *38*, 97. (f) Pecoraro, V. L. *Manganese Redox Enzymes*; Verlag Chemie: New York, 1992. (g) Pecoraro, V. L.; Baldwin, M. J.; Gelasco, A. *Chem. Rev.* **1994**, *94*, 807.

(2) (a) Yachandra, V. K.; DeRose, V. J.; Latimer, M. J.; Mukerji, I.; Sauer, K.; Klein, M. P. *Science* **1993**, *260*, 675. (b) DeRose, V. J.; Mukerji, I.; Latimer, M. J.; Yachandra, V. K.; Sauer, K.; Klein, M. P. *J. Am. Chem. Soc.* **1994**, *116*, 5239.

(3) (a) Kono, Y.; Fridovich, I. *J. Biol. Chem.* **1983**, *258*, 6015. (b) Beyer, W. F., Jr.; Fridovich, I. *Biochemistry* **1985**, *24*, 6460. (c) Waldo, G. S.; Fronko, R. M.; Penner-Hahn, J. E. *Biochemistry* **1991**, *30*, 10486. (d) Waldo, G. S.; Yu, S.; Penner-Hahn, J. E. *J. Am. Chem. Soc.* **1992**, *114*, 5869. (e) Penner-Hahn, J. E. In *Manganese Redox Enzymes*; Pecoraro, V. L., Ed.; Verlag Chemie: New York, 1992; p 29. (f) Waldo, G. S.; Penner-Hahn, J. E. *Biochemistry* **1995**, *34*, 1507.

(4) (a) Barynin, V. V.; Vagin, A. A.; Melik-Adamyan, V. R.; Grebenko, A. I.; Khangulov, S. V.; Popov, A. N.; Andrianova, M. E.; Vainshtein, B. K. *Dokl. Akad. Nauk. SSSR* **1986**, *288*, 877. (b) Khangulov, S. V.; Barynin, V. V.; Voevodskaya, N. V.; Grebenko, A. I. *Biochim. Biophys. Acta* **1990**, *1020*, 305.

(5) (a) Dismukes, G. C. In *Bioinorganic Catalysis*; Reedijk, J., Ed.; Marcel Dekker: Amsterdam, 1992. (b) Khangulov, S. V.; Goldfeld, M. G.; Gerasimenko, V. V.; Andreeva, N. E.; Barynin, V. V.; Grebenko, A. I. *J. Inorg. Biochem.* **1990**, *40*, 279.

0020-1669/95/1334-4682$09.00/0 © 1995 American Chemical Society

manganese(II or III)[7] have also been reported. An X-ray crystal structure analysis[8] of the Mn(II)-substituted RR from *Escherichia coli* has shown that two Mn(II) ions are bridged by two carboxylate groups of glutamate residues at a separation of 3.6 Å. The remaining terminal positions of each metal center are occupied by histidine residues and a monodentate carboxylate group, with a water molecule coordinated to one of the Mn(II) atoms. The native manganese-containing RR[9] from the gram-positive *Brevibacterium ammoniagenes* is believed to have a dimetallic active site structure similar to that in the iron-containing RR.[10] Furthermore, recent biological studies have revealed that carboxylate-bridged dimanganese(II) units play critical roles in non-redox active metalloenzymes such as arginase,[11] enolase,[12] ribonuclease H of HIV 1 reverse transcriptase,[13] inorganic pyrophosphatase from *Saccharomyces cerevisiae*,[14] DNA polymerase I from *E. coli*,[15] fructose-1,6-bisphosphatase,[16] and xylose isomerases.[17]

Because of the biological importance of di- and polynuclear manganese centers, several low molecular weight model complexes have been prepared and characterized to model their structures, physical properties, and catalytic activity.[1,18] The first generation of such models were composed of (μ-oxo)bis(μ-carboxylato)dimanganese(III) complexes with two tridentate N-donor ligands capping each end of the molecule, examples being hydrotris(pyrazol-1-yl)borate ($HB(pz)_3$),[19] 1,4,7-triazacyclononane (tacn) and 1,4,7-trimethyl-1,4,7-triazacyclononane (Me_3tacn),[20] and tris(*N*-methylimidazol-2-yl)phosphine (TMIP).[21] The tridentate capping ligands were employed in part to prevent polymeric cluster formation, thus facilitating self-assembly of the dinuclear core. This strategy blocks all terminal coordination sites from access to substrates, however, resulting in poor catalytic activities. Related (μ-oxo)bis(μ-carboxylato)dimanganese(III) complexes with bidentate 2,2′-dipyridyl (bpy) terminal ligands were reported as models for manganese catalase enzymes. In these compounds, terminal coordination sites are available for binding additional ligands such as Cl^-, N_3^-, H_2O, and $S_2O_8^-$.[22,23] In contrast to these dimanganese(III) complexes, effective self-assembly routes to carboxylate-bridged dimanganese(II) compounds are rather limited owing to the lability of Mn(II) ions and its propensity to undergo both substitution and redox reactions. Structurally characterized examples are $[Mn_2(\mu\text{-}OH)(\mu\text{-}OAc)_2(Me_3tacn)_2]^+$, $[Mn_2(\mu\text{-}OAc)_3(Me_3tacn)_2]^+$,[20] $[Mn_2(\mu\text{-}C_3F_7CO_2)_4(bpy)_2]$,[1a] $[Mn_2(\mu\text{-}OAc)_3(bpy)_2(ClO_4)]$, $[Mn_2(\mu\text{-}OAc)_2(bpy)_4](ClO_4)_2$,[24] $[Mn_2(\mu\text{-}OAc)_2L_2](ClO_4)_2$ (L = *N*,*N*′-dimethyl-*N*,*N*′-bis(2-pyridylmethyl)ethane-1,2-diamine),[25] $[Mn_2\{HB(3,5\text{-}{}^iPr_2pz)_3\}(\mu\text{-}BzO)_3(3,5\text{-}{}^iPr_2pzH)_2]$,[26] and carboxylate-bridged Mn(II) complexes with μ-alkoxo- or μ-phenoxo-based dinucleating ligands.[6,27,28]

Recently we reported the synthesis and characterization of dinuclear Mn(II) complexes with water and carboxylate bridges, $[Mn_2(\mu\text{-}H_2O)(\mu\text{-}{}^t BuCO_2)_2({}^t BuCO_2)_2(4,4'\text{-}Me_2bpy)_2]$ and $[Mn_2(\mu\text{-}H_2O)(\mu\text{-}OAc)_2(OAc)_2(tmen)_2]$ (4,4′-Me_2bpy = 4,4′-dimethyl-2,2′-dipyridyl, tmen = *N*,*N*,*N*′,*N*′-tetramethylethylenediamine).[29] In the present article, we describe a facile synthesis of a bis(μ-carboxylato)dimanganese(II) complex with labile solvent molecules and a nitrate anion in the terminal positions, $[Mn_2(XDK)(NO_3)(H_2O)_2(CH_3OH)_4](NO_3)$ (**1**), by using the remarkable dinucleating ligand XDK, H_2XDK = *m*-xylenediamine bis(Kemp's triacid imide).[30] XDK has already been shown to be effective for preparing homodinuclear Fe(II), Fe(III), Co(II), Zn(II), and Mg(II), as well as a series of heterodinuclear $Zn^{II}M^{II}$ (M = Ni, Co, Fe, Mn) complexes.[31,32] As described here, **1** readily undergoes terminal ligand exchange reactions with N-donor bidentate ligands and could be further oxidized by *tert*-butyl hydroperoxide to afford the (μ-oxo)bis(μ-carboxylato)dimanganese(III) complexes. Finally, we report its decomposition in the presence of hydrogen peroxide to MnO_2, which efficiently catalyzes the disproportionation of H_2O_2 in a heterogeneous manner. This last result should be of interest to investigators working to develop manganese catalase model systems.

(6) (a) Pessiki, P. J.; Khangulov, S. V.; Ho, D. M.; Dismukes, G. C. *J. Am. Chem. Soc.* **1994**, *116*, 891. (b) Pessiki, P. J.; Dismukes, G. C. *J. Am. Chem. Soc.* **1994**, *116*, 898.
(7) Gelasco, A.; Pecoraro, V. L. *J. Am. Chem. Soc.* **1993**, *115*, 7928.
(8) Atta, M.; Nordlund, P.; Åberg, A.; Eklund, H.; Fontecave, M. *J. Biol. Chem.* **1992**, *267*, 20682.
(9) Willing, A.; Follmann, H.; Auling, G. *Eur. J. Biochem.* **1988**, *170*, 603.
(10) Nordlund, P.; Eklund, H.; Sjöberg, B.-M.; Eklund, H. *Nature* **1990**, *345*, 593.
(11) Reczkowski, R. S.; Ash, D. E. *J. Am. Chem. Soc.* **1992**, *114*, 10992.
(12) Poyner, R. R.; Reed, G. H. *Biochemistry* **1992**, *31*, 7166.
(13) Davies, J. F.; Hostomska, Z.; Hostomsky, Z.; Jordan, S. R.; Matthews, D. A. *Science* **1991**, *252*, 88.
(14) Cooperman, B. S.; Baykov, A. A.; Lahti, R. *Trends Biochem. Sci.* **1992**, *17*, 262.
(15) (a) Beese, L. S.; Steitz, T. A. *EMBO J.* **1991**, *10*, 25. (b) Freemont, P. S.; Friedman, J. M.; Beese, L. S.; Sanderson, M. R.; Steitz, T. A. *Proc. Natl. Acad. Sci. U.S.A.* **1988**, *85*, 8924. (c) Beese, L. S.; Friedman, J. M.; Steitz, T. A. *Biochemistry* **1993**, *32*, 14095.
(16) Zhang, Y.; Liang, J.-Y.; Huang, S.; Ke, H.; Lipscomb, W. N. *Biochemistry* **1993**, *32*, 1844.
(17) (a) Jenkins, J.; Janin, J.; Rey, F.; Chiadmi, M.; Tilbeurgh, H.; Lasters, I.; Maeyer, M. D.; Belle, D. V.; Wodak, S. J.; Lauwereys, M.; Stanssens, P.; Mrabet, N. T.; Snauwaert, J.; Matthyssens, G.; Lambeir, A.-M. *Biochemistry* **1992**, *31*, 5449. (b) Whitlow, M.; Howard, A. J.; Finzel, B. C.; Poulos, T. L.; Winborne, E.; Gilliland, G. L. *Proteins* **1991**, *9*, 153.
(18) Rardin, R. L.; Tolman, W. B.; Lippard, S. J. *New J. Chem.* **1991**, *15*, 417.
(19) Sheats, J. E.; Czernuszewicz, R. S.; Dismukes, G. C.; Rheingold, A. L.; Petrouleas, V.; Stubbe, J.; Armstrong, W. H.; Beer, R. H.; Lippard, S. J. *J. Am. Chem. Soc.* **1987**, *109*, 1435.
(20) (a) Wieghardt, K.; Bossek, U.; Ventur, D.; Weiss, J. *J. Chem. Soc., Chem. Commun.* **1985**, 347. (b) Wieghardt, K.; Bossek, U.; Nuber, B.; Weiss, J.; Bonvoisin, J.; Corbella, M.; Vitols, S. E.; Girerd, J. J. *J. Am. Chem. Soc.* **1988**, *110*, 7398. (c) Bossek, U.; Wieghardt, K.; Nuber, B.; Weiss, J. *Inorg. Chim. Acta* **1989**, *165*, 123.
(21) Wu, F.-J.; Kurtz, D. M. J.; Hagen, K. S.; Nyman, P. D.; Debrunner, P. G.; Vankai, V. A. *Inorg. Chem.* **1990**, *29*, 5174.
(22) Menage, S.; Girerd, J.-J.; Gleizes, A. *J. Chem. Soc., Chem. Commun.* **1988**, 431.
(23) (a) Vincent, J. B.; Tsai, H.-L.; Blackman, A. G.; Wang, S.; Boyd, P. D. W.; Folting, K.; Huffman, J. C.; Lobkovsky, E. B.; Hendrickson, D. N.; Christou, G. *J. Am. Chem. Soc.* **1993**, *115*, 12353. (b) Blackman, A. G.; Huffman, J. C.; Lobkovsky, E. B.; Christou, G. *J. Chem. Soc., Chem. Commun.* **1991**, 989.
(24) Christou, G. Private communication, cited in ref 18.
(25) Che, C.-M.; Tang, W.-T.; Wong, K.-Y.; Wong, W.-T.; Lai, T.-F. *J. Chem. Res. (S)* **1991**, 30.
(26) Osawa, M.; Singh, U. P.; Tanaka, M.; Moro-oka, Y.; Kitajima, N. *J. Chem. Soc., Chem. Commun.* **1993**, 310.
(27) Gultneh, Y.; Farooq, A.; Liu, S.; Karlin, K. D.; Zubieta, J. *Inorg. Chem.* **1992**, *31*, 3607.
(28) (a) Sakiyama, H.; Okawa, H.; Isobe, R. *J. Chem. Soc., Chem. Commun.* **1993**, 882. (b) Higuchi, C.; Sakiyama, H.; Okawa, H.; Isobe, R.; Fenton, D. E. *J. Chem. Soc., Dalton Trans.* **1994**, 1097.
(29) Yu, S.-B.; Lippard, S. J.; Shweky, I.; Bino, A. *Inorg. Chem.* **1992**, *31*, 3502.
(30) Rebek, J., Jr.; Marshall, L.; Wolak, R.; Parris, K.; Killoran, M.; Askew, B.; Nemeth, D.; Islam, N. *J. Am. Chem. Soc.* **1985**, *107*, 7476.
(31) (a) Goldberg, D. P.; Watton, S. P.; Masschelein, A.; Wimmer, L.; Lippard, S. J. *J. Am. Chem. Soc.* **1993**, *115*, 5346. (b) Watton, S. P.; Masschelein, A.; Rebek, J., Jr.; Lippard, S. J. *J. Am. Chem. Soc.* **1994**, *116*, 5196. (c) Tanase, T.; Watton, S. P.; Lippard, S. J. *J. Am. Chem. Soc.* **1994**, *116*, 9401. (d) Tanase, T.; Yun, J. W.; Lippard, S. J. *Inorg. Chem.*, in press. (e) Yun, J. W.; Tanase, T.; Pence, L. E.; Lippard, S. J. *J. Am. Chem. Soc.* **1995**, *117*, 4407.
(32) (a) Hagen, K. S.; Lachicotte, R.; Kitaygorodskiy, A.; Elbouadili, A. *Angew. Chem., Int. Ed. Engl.* **1993**, *32*, 1321. (b) Hagen, K. S.; Lachicotte, R.; Kitaygorodskiy, A. *J. Am. Chem. Soc.* **1993**, *115*, 12617.

Experimental Section

All experiments except for the preparation of **3** were carried out in the air, and all reagents and solvents were used as received. *m*-Xylenediamine bis(Kemp's triacid imide) (H_2XDK) was prepared by a known method[30] and recrystallized from CH_2Cl_2/Et_2O.

Physical Measurements. Infrared and electronic absorption spectra were recorded on BIO-RAD SPC 3200 and Perkin-Elmer Lambda 7 spectrometers, respectively. ^1H NMR spectra were measured at 250 MHz on a Bruker AC250 instrument. Molar conductivities were recorded at 24 °C in methanol by using a Fisher Scientific Model 9-326 conductivity bridge and a platinum-black electrode. Conductivities were recorded over a concentration range of 0.4−2.5 mM, and the reported molar conductivities (Ω^{-1} cm^2 mol^{-1}) were derived from the slopes of linear plots of conductivity (Ω^{-1} cm^{-1}) *vs* concentration (mol cm^{-3}). The type of electrolyte (1:1, 2:1) was estimated by comparison to the concentration-dependent molar conductivity curve for the reference 1:1 electrolyte, ($^nBu_4N$)(PF_6). Cyclic voltammetry was performed with a Princeton Applied Research Model 263 potentiostat and potential scanning unit with the operating program ECHEM. The electrolytic cell consisted of a conventional three-electrode system, a platinum-button (~3 mm^2) working electrode, a platinum-wire counter electrode, and a 0.1 M Ag/$AgNO_3$ in CH_3CN reference electrode. Experiments were carried out on 5 mM DMF solutions of complexes **2** and **5** at room temperature under a nitrogen atmosphere, and 0.1 M ($^nBu_4N$)(PF_6) was used as supporting electrolyte.

Preparation of $Na_2XDK·4H_2O$. To a suspension of H_2XDK (1.84 g, 3.17 mmol) in methanol (100 mL) was added 20 mL of a methanolic solution of NaOH (0.36 M, 7.2 mmol). The reaction mixture was stirred at room temperature for 30 min, after which time the H_2XDK had dissolved. The solvent was removed with a rotary evaporator to give colorless crystals of $Na_2XDK·4H_2O$, which were collected, washed with Et_2O, and dried in vacuo (1.58 g, 72%). Anal. Calcd for $C_{32}H_{46}N_2O_{12}Na_2$: C, 55.17; H, 6.65; N, 4.02. Found: C, 55.50; H, 6.41; N, 4.07. IR (Nujol): 3500 (br), 3369 (br), 1731, 1675 (s), 1586 (s), 1196 (s), 1029, 958, 886, 852, 760, 721 cm^{-1}. $Na_2XDK·4H_2O$ can be recrystallized from a minimum amount of CH_3OH.

Preparation of $[Mn_2(XDK)(NO_3)(CH_3OH)_4(H_2O)_2](NO_3)$ (1). $Na_2XDK·4H_2O$ (240 mg, 0.344 mmol) was added to a solution of $Mn(NO_3)_2·6H_2O$ (221 mg, 0.770 mmol) in methanol (30 mL). The solution was stirred at room temperature for 30 min. Pyridine (1.5 mL) was added to the solution, and the reaction mixture was stirred for another 30 min. The solution was concentrated to dryness, and the residue was extracted with 20 mL of methylene chloride. The extract was passed through a glass filter to remove inorganic salts and was concentrated again to dryness. The residue was crystallized from a MeOH (2 mL)/Et_2O (5 mL)/*n*-hexane (0.5 mL) mixed solvent system at −20 °C to afford colorless crystals of $[Mn_2(XDK)(NO_3)(CH_3OH)_4(H_2O)_2](NO_3)$ (**1**), which were collected, washed with Et_2O, and dried in vacuo (316 mg, 96% based on XDK). Anal. Calcd for $C_{36}H_{58}N_4O_{20}Mn_2$: C, 44.27; H, 5.99; N, 5.74. Found: C, 44.10; H, 5.90; N, 5.62. IR (Nujol): 3412 (br), 1716, 1677 (s), 1603, 1310, 1192 (s), 959, 851, 765, 722 cm^{-1}. Recrystallization of **1** from MeOH/Et_2O/*n*-hexane at room temperature gave block-shaped crystals suitable for X-ray crystallography.

Preparation of $[Mn_2(XDK)L_2(NO_3)_2(H_2O)]$ (L = bpy (2), 4,4′-Me_2bpy (3), and phen (4)). Compound **1** (100 mg, 0.102 mmol) was dissolved in CH_3OH (10 mL)/CH_2Cl_2 (2 mL) to which 2,2′-dipyridyl (bpy) (39 mg, 0.25 mmol) had been added. The color of the solution changed from colorless to pale yellow, and the reaction solution was stirred at room temperature for 30 min. The solvent was removed, and the residue was extracted with 2 mL of CH_2Cl_2. An addition of Et_2O (1 mL) to the CH_2Cl_2 solution gave pale yellow crystals of $[Mn_2(XDK)(bpy)_2(NO_3)_2(H_2O)]·1.5CH_2Cl_2$ (**2**·1.5CH_2Cl_2), which were collected, washed with Et_2O, and dried in vacuo (113 mg, 87%). Anal. Calcd for $C_{53.5}H_{59}N_8O_{15}Mn_2Cl_3$: C, 50.58; H, 4.68; N, 8.82. Found: C, 50.55; H, 4.63; N, 8.86. IR (Nujol): 3511 (br), 1726, 1676 (s), 1595, 1378 (s), 1300, 1197 (s), 1016, 959, 889, 851, 821, 776, 765 (s), 733 (s), 701 cm^{-1}. Recrystallization of **2** from a concentrated CH_2Cl_2/Et_2O solution afforded block-shaped crystals of **2**·CH_2Cl_2 which were suitable for X-ray crystallography. Similar procedures using 4,4′-dimethyl-2,2′-dipyridyl (4,4′-Me_2bpy) and 1,10-phenanthroline (phen) gave $[Mn_2(XDK)(4,4'\text{-}Me_2bpy)_2(NO_3)_2(H_2O)]$ (**3**, 89%) and $[Mn_2(XDK)(phen)_2(NO_3)_2(H_2O)]·CH_2Cl_2$ (**4**·CH_2Cl_2, 91%), respectively. The preparation of **3** was carried out under a nitrogen atmosphere to avoid air oxidation of the product. Anal. Calcd for $C_{56}H_{64}N_8O_{15}Mn_2$ (**3**): C, 56.10; H, 5.38; N, 9.35. Found: C, 55.91; H, 5.62; N, 8.93. IR (Nujol): 3500 (br), 1720, 1670 (s), 1590, 1370 (s), 1300, 1190 (s), 1010, 950, 880, 850, 820, 770, 760 (s), 730 (s), 700 cm^{-1}. Anal. Calcd for $C_{57}H_{58}N_8O_{15}Mn_2Cl_2$ (**4**·CH_2Cl_2): C, 53.66; H, 4.58; N, 8.78. Found: C, 54.08; H, 5.03; N, 9.11. IR (Nujol): 3484 (br), 1721, 1682 (s), 1601 (s), 1293 (s), 1198 (s), 959, 887, 852, 774, 761 (s), 738 (s), 722 cm^{-1}.

Preparation of $[Mn_2(\mu\text{-}O)(XDK)L_2(NO_3)_2]$ (L = bpy (5) and 4,4′-Me_2bpy (6)). A 20 mL methanolic solution of $[Mn_2(XDK)(bpy)_2(NO_3)_2(H_2O)]$ (**2**) was prepared by reacting $[Mn_2(XDK)(NO_3)(CH_3OH)_4(H_2O)_2](NO_3)$ (**1**) (160 mg, 0.164 mmol) with bpy (62 mg, 0.40 mmol). To the solution was added 100 μL of *tert*-butyl hydroperoxide (TBHP) (70% aqueous solution, ~0.78 mmol) at room temperature. The color of the solution immediately changed from pale yellow to dark violet. After 30 min, the solution was concentrated to ca. 5 mL; addition of Et_2O (2 mL) yielded violet crystals of $[Mn_2(\mu\text{-}O)(XDK)(bpy)_2(NO_3)_2]·CH_3OH·2H_2O$ (**5**·$CH_3OH·2H_2O$), which were collected by filtration, washed with Et_2O, and dried in vacuo (132 mg, 67%). Anal. Calcd for $C_{53}H_{62}N_8O_{18}Mn_2$: C, 52.65; H, 5.17; N, 9.27. Found: C, 52.59; H, 5.12; N, 9.34. IR (Nujol): 3404 (br), 1731, 1683 (s), 1586, 1559, 1336, 1316, 1303, 1191 (s), 1034 (s), 959, 889, 730 (s), 722 (s, br) cm^{-1}. UV/vis (CH_3OH) [λ_{max} (ϵ, M^{-1} cm^{-1} metal^{-1})]: 442 (sh, 134), 500 (140), 520 (sh, 130), 574 (sh, 88), 696 (80) nm. A similar procedure with 4,4′-Me_2bpy afforded $[Mn_2(\mu\text{-}O)(XDK)(4,4'\text{-}Me_2bpy)_2(NO_3)_2]·CH_3OH$ (**6**·CH_3OH) in 84% yield. Anal. Calcd for $C_{57}H_{66}N_8O_{16}Mn_2$: C, 55.70; H, 5.41; N, 9.12. Found: C, 55.54; H, 5.36; N, 9.36. IR (Nujol): 3400 (br), 1728, 1684 (s), 1617 (s), 1585 (s), 1559, 1302, 1187 (s), 1032 (s), 959, 923, 851, 831, 721 (s, br) cm^{-1}. UV/vis (CH_3OH) [λ_{max} (ϵ, M^{-1} cm^{-1} metal^{-1})]: 432 (sh, 179), 500 (218), 530 (sh, 204), 572 (sh, 140), 698 (141) nm. Vapor diffusion of Et_2O into a concentrated methanolic solution of **6**·CH_3OH afforded violet-green dichroic rectangular crystals of **6**·2.5CH_3OH.

Preparation of $[Mn(HXDK)_2(H_2O)_2]$ (7). To a methanolic solution (30 mL) of $Mn(NO_3)_2·6H_2O$ (83 mg, 0.286 mmol) were added H_2XDK (322 mg, 0.572 mmol) and NaOH (0.57 mmol in methanol). The solution was stirred at room temperature for 30 min to give a white precipitate, which was filtered, washed with Et_2O, and dried in vacuo. $[Mn(HXDK)_2(H_2O)_2]$ (**7**) was obtained in 42% yield (151 mg). Anal. Calcd for $C_{64}H_{82}N_2O_{18}Mn$: C, 61.48; H, 6.61; N, 4.48. Found: C, 61.75; H, 6.65; N, 4.55. IR (Nujol): 3354, 1738, 1694 (s), 1668, 1633, 1195, 1034, 956 cm^{-1}.

Disproportionation of Hydrogen Peroxide. Experiments were carried out in methanol (20 mL) at 24 °C using a 30% aqueous H_2O_2 solution (10 mmol). The time course of dioxygen evolution was monitored by a gas buret containing O_2-saturated mineral oil. The following systems were examined: **1** (40 μmol), **1** (40 μmol) + bpy (80 μmol), **1** (40 μmol) + 4,4′-Me_2bpy (80 μmol), **1** (40 μmol) + phen (80 μmol), and $Mn(NO_3)_2·6H_2O$ (80 μmol).

X-ray Crystallographic Analyses of $[Mn_2(XDK)(NO_3)(CH_3OH)_4(H_2O)_2](NO_3)$ (1), $[Mn_2(XDK)(bpy)_2(NO_3)_2(H_2O)]·CH_2Cl_2$ (2·CH_2Cl_2), and $[Mn_2(\mu\text{-}O)(XDK)(4,4'\text{-}Me_2bpy)_2(NO_3)_2]·2.5CH_3OH$ (6·2.5CH_3OH). Crystal data and experimental conditions are listed in Table 1. All data were collected at −74 °C on an Enraf-Nonius CAD4 diffractometer equipped with graphite-monochromatized Mo Kα (λ = 0.710 69 Å) radiation. Three standard reflections were monitored every ~200 reflections and showed no systematic decrease in intensity. Reflection data were corrected for Lorentz−polarization and absorption effects.

Structure Solution and Refinement. $[Mn_2(XDK)(NO_3)(CH_3OH)_4(H_2O)_2](NO_3)$ (1) and $[Mn_2(XDK)(NO_3)_2(H_2O)]·CH_2Cl_2$ (2·CH_2Cl_2). The structures were solved by direct methods with SIR92.[33] The two Mn atoms and most atoms of XDK, the nitrates, and other ligands were located initially, and subsequent cycles of full-matrix least-square refinement and difference Fourier syntheses gave the positions of remaining non-hydrogen atoms. The coordinates of all carbon-bound hydrogen atoms were calculated at ideal positions with d_{C-H} = 0.95

(33) Burla, M. C.; Camalli, M.; Cascarano, C.; Giacovazzo, C.; Polidori, G.; Spagna, R.; Viterbo, D. *J. Appl. Crystallogr.* **1989**, *22*, 389.

Table 1. Crystallographic Data for $[Mn_2(XDK)(NO_3)(CH_3OH)_4(H_2O)_2](NO_3)$ (**1**), $[Mn_2(XDK)(bpy)_2(NO_3)_2(H_2O)]\cdot CH_2Cl_2$ (**2**·CH_2Cl_2), and $[Mn_2(\mu\text{-}O)(XDK)(4,4'\text{-}Me_2bpy)_2(NO_3)_2]\cdot 2.5CH_3OH$ (**6**·2.5CH_3OH)

compd	**1**	**2**·CH_2Cl_2	**6**·2.5CH_3OH
formula	$C_{36}H_{58}N_4O_{20}Mn_2$	$C_{53}H_{58}N_8O_{15}Mn_2Cl_2$	$C_{58.5}H_{72}N_8O_{17.5}Mn_2$
fw	976.74	1227.87	1277.13
cryst system	monoclinic	monoclinic	orthorhombic
space group	$P2_1/c$ (No. 14)	$P2_1/c$ (No. 14)	*Pbcn* (No. 60)
a, Å	11.226(1)	14.491(2)	41.636(9)
b, Å	13.120(1)	17.945(2)	13.108(1)
c, Å	30.467(3)	22.492(3)	22.422(9)
β, deg	98.739(8)	108.787(9)	
V, Å^3	4435.2(7)	5537(1)	12237(2)
Z	4	4	8
T, °C	−74	−74	−74
D_{calcd}, g cm^{-3}	1.463	1.473	1.386
abs coeff, cm^{-1}	6.51	6.27	4.89
trans factor	0.97−1.00	0.93−1.00	0.56−1.00
2θ range, deg	$3 < 2\theta < 46$	$3 < 2\theta < 48$	$3 < 2\theta < 45$
no. of unique data	6472	8992	8789
no. of obsd data ($I > 3\sigma(I)$)	4957	4438	3731
no. of variables	560	722	593
R^a	0.034	0.055	0.073
$R_w{}^a$	0.045	0.058	0.085

^{a} $R = \sum||F_o| - |F_c||/\sum|F_o|$; $R_w = [\sum w(|F_o| - |F_c|)^2/\sum w|F_o|^2]^{1/2}$ ($w = 1/\sigma^2(F_o)$). More details about the weighting scheme and other experimental protocols may be found in: Carnahan, E. M.; Rardin, R. L.; Bott, S. G.; Lippard, S. J. *Inorg. Chem.* **1992**, *31*, 5193.

Å, and those of oxygen-bound hydrogen atoms (H_2O and MeOH) were determined by difference Fourier syntheses. All hydrogen atoms were fixed with an appropriate B_{iso} during refinement. The structure was refined by full-matrix least-square techniques minimizing $\sum w(|F_o| - |F_c|)^2$. Final refinement with anisotropic thermal parameters for non-hydrogen atoms converged to $R = 0.034$ and $R_w = 0.045$ for **1** and $R = 0.055$ and $R_w = 0.058$ for **2**·CH_2Cl_2, where $R = \sum||F_o| - |F_c||/\sum|F_o|$ and $R_w = [\sum w(|F_o| - |F_c|)^2/\sum w|F_o|^2]^{1/2}$ ($w = 1/\sigma^2(F_o)$).

$[Mn_2(\mu\text{-}O)(XDK)(4,4'\text{-}Me_2bpy)_2(NO_3)_2]\cdot 2.5CH_3OH$ (6·2.5CH_3OH). The structure was solved and refined by procedures similar to those described above. The positions of all hydrogen atoms except for those of solvent molecules were calculated and not refined. Final refinement with anisotropic thermal parameters for non-hydrogen atoms (the carbon atoms of XDK were refined isotropically) converged at $R = 0.073$ and $R_w = 0.085$. A disordered, half-methanol solvent molecule was refined as follows: an oxygen atom was assigned with 0.5 occupancy and connected to the carbon atom which resides on a special position at ($^1/_2$, y, $^1/_4$) with 0.5 occupancy.

Atomic scattering factors and values of f' and f'' for Mn, Cl, O, N, and C were taken from the literature.[34] All calculations were carried out on a Digital Equipment VAX Station 3100 or 4200 with the TEXSAN Program System.[35] Perspective views were drawn by using the program ORTEP.[36] Selected final atomic parameters for non-hydrogen atoms of compounds **1**, **2**·CH_2Cl_2, and **6**·2.5CH_3OH are listed in Table 2. A complete compilation of final parameters for all atoms is supplied as supporting information.

Results and Discussion

Synthesis and Solution Properties of Dinuclear Mn(II) XDK Complexes. Despite increased recognition of their importance in many biological systems, synthetic routes to carboxylate-bridged dimanganese(II) complexes are relatively few in number.[1,11-17] Recently we have established that carboxylate-bridged dinuclear complexes with solvent molecules coordinated to the terminal positions of labile metal ions can be accessed by using the cleft-shaped dicarboxylate ligand XDK. Complexes $[Fe_2(\mu\text{-}O)(XDK)(CH_3OH)_5(H_2O)](NO_3)_2$,[31b] $[Zn_2(XDK)(NO_3)_2(CH_3OH)(H_2O)_2]$,[31d] and $[Mg_2(XDK)(NO_3)(CH_3OH)_4(H_2O)](NO_3)$[31e] were shown to be good precursors for introduction of N-donor ligands such as bpy, py, and 1-methylimidazole, as well as organic phosphate esters, into the dinuclear core. In the present study, this methodology was applied to the synthesis of dinuclear Mn(II) complexes, from which it was clearly revealed that XDK acts as an efficient dinucleating ligand for assembling complexes having the labile dimanganese(II) core.

The reaction of $Mn(NO_3)_2\cdot 6H_2O$ (2 equiv) with $Na_2XDK\cdot 4H_2O$ (1 equiv) in methanol and the subsequent purification by using pyridine afforded $[Mn_2(XDK)(NO_3)(CH_3OH)_4(H_2O)_2](NO_3)$ (**1**) in quantitative yield. The IR spectrum revealed the presence of XDK (1726−1595 cm^{-1}), nitrate anions (1319−1300 cm^{-1}), and hydroxyl groups of water and methanol (~3500 cm^{-1}). The molar conductivity of 141 Ω^{-1} cm^2 mol^{-1} in methanol at 24 °C fell within the range expected for a 1:2 electrolyte, indicating that the nitrate anion is dissociated from the dinuclear center in this solvent. Compound **1** dissolved in methanol is stable in air but is oxidized in the presence of bases such as hydroxide and aliphatic amines to give MnO_2 as a brown precipitate.

Pale yellow complexes of general formula $[Mn_2(XDK)L_2(NO_3)_2(H_2O)]$ (L = bpy (**2**), 4,4′-Me_2bpy (**3**), and phen (**4**)) were obtained in high yields in the reaction of **1** with 2 equiv or an excess of N-donor bidentate ligands (L). As was the case for **1**, the IR spectra of **2**−**4** showed the presence of XDK, nitrate anions, and water, as well as peaks for the N-donor ligands. The molar conductivity of **2** in methanol was 145 Ω^{-1} cm^2 mol^{-1}, consistent with the nitrate anions being replaced by solvent molecules, resulting in a 1:2 electrolyte. The cyclic voltammogram of **2** did not show any redox processes within the DMF solvent window (−2.0 to 1.5 V), demonstrating its unusual stability toward oxidation.

Structure of $[Mn_2(XDK)(NO_3)(CH_3OH)_4(H_2O)_2](NO_3)$ (1). Drawings of the complex cation of **1** with its atomic labeling scheme are given in Figures 1a,b. Selected bond lengths and angles are listed in Table 3. The complex consists of a bis(μ-carboxylato)dimanganese(II) core with a bridging XDK ligand. The two Mn atoms are not supported by any additional bridge other than XDK. The nonbonding interatomic Mn···Mn distance is 4.8497(7) Å, remarkably longer than those found in $[Mn^{II}_2L_2(\mu\text{-}OAc)_2](ClO_4)_2$ (4.298 Å)[25] (L = *N*,*N*′-dimethyl-

(34) (a) Cromer, D. T.; Waber, J. T. In *International Tables for X-ray Crystallography*; Kynoch Press: Birmingham, England, 1974; Vol. IV. (b) Cromer, D. T. *Acta Crystallogr.* **1965**, *18*, 17.
(35) TEXSAN Structure Analysis Package, Molecular Structure Corp., The Woodlands, TX, 1985.
(36) Johnson, C. K. ORTEP-II, Oak Ridge National Laboratory, Oak Ridge, TN, 1976.

Table 2. Atomic Positional and Thermal Parameters (Å^2) for Coordination Spheres in **1**, **2**·CH_2Cl_2, and **6**·2.5CH_3OH[a,b]

atom	x	y	z	B_{eq}	atom	x	y	z	B_{eq}
				$[Mn_2(XDK)(NO_3)(CH_3OH)_4(H_2O)_2](NO_3)$ (**1**)					
Mn(1)	1.47490(4)	0.09713(4)	0.91067(2)	1.86(2)	O(201)	1.2927(2)	0.0865(2)	0.90892(7)	2.6(1)
Mn(2)	1.16910(4)	0.35655(4)	0.91491(2)	1.87(2)	O(202)	1.1444(2)	0.1966(2)	0.91321(7)	2.4(1)
O(1)	1.2436(2)	0.3586(2)	0.98529(7)	3.0(1)	N(11)	1.6349(3)	0.1509(2)	0.9815(1)	3.0(1)
O(2)	0.9938(2)	0.3796(2)	0.93829(8)	3.4(1)	N(101)	1.3969(2)	0.3407(2)	0.79606(8)	1.8(1)
O(3)	1.1625(2)	0.5253(2)	0.91168(7)	2.9(1)	N(201)	1.1048(2)	0.0748(2)	0.81819(8)	1.8(1)
O(4)	1.0794(2)	0.3726(2)	0.84659(7)	2.3(1)	C(1)	1.3383(4)	0.2917(3)	1.0029(1)	3.8(2)
O(5)	1.5046(2)	−0.0643(2)	0.92864(7)	2.9(1)	C(2)	0.9263(4)	0.3115(3)	0.9597(2)	5.1(2)
O(6)	1.4790(2)	0.0536(2)	0.84183(7)	2.3(1)	C(3)	1.2298(4)	0.5945(3)	0.9408(1)	4.4(2)
O(11)	1.5269(2)	0.1215(2)	0.98454(7)	2.7(1)	C(4)	1.4954(4)	−0.1528(3)	0.9016(1)	4.0(2)
O(12)	1.6709(2)	0.1349(2)	0.94538(8)	3.4(1)	C(101)	1.4482(3)	0.3401(2)	0.8937(1)	1.9(1)
O(13)	1.6959(3)	0.1939(2)	1.01259(9)	4.9(1)	C(107)	1.5400(3)	0.4260(2)	0.8909(1)	2.3(1)
O(101)	1.4858(2)	0.2504(2)	0.89317(7)	2.5(1)	C(201)	1.1867(3)	0.1089(2)	0.9135(1)	1.9(1)
O(102)	1.3439(2)	0.3652(2)	0.89858(7)	2.5(1)	C(207)	1.1051(3)	0.0201(2)	0.9234(1)	2.2(1)
				$[Mn_2(XDK)(bpy)_2(NO_3)_2(H_2O)]$·$CH_2Cl_2$ (**2**·CH_2Cl_2)					
Mn(1)	1.33626(8)	−0.07712(6)	1.25271(5)	1.90(4)	N(11)	1.3203(4)	−0.1368(3)	1.1624(3)	2.3(3)
Mn(2)	1.17190(8)	−0.28263(6)	1.28276(5)	2.36(5)	N(12)	1.4800(4)	−0.0626(3)	1.2296(3)	2.0(2)
O(11)	1.2868(4)	0.0232(3)	1.1909(3)	4.6(3)	N(21)	1.0137(4)	−0.3021(3)	1.2720(3)	2.3(3)
O(12)	1.1900(4)	0.0506(3)	1.0921(2)	4.0(3)	N(22)	1.1665(5)	−0.3526(3)	1.3634(3)	3.4(3)
O(13)	1.1420(5)	−0.0358(4)	1.1412(3)	5.5(3)	N(31)	1.2056(6)	0.0113(4)	1.1401(4)	4.9(4)
O(21)	1.1318(4)	−0.2948(3)	1.1802(3)	4.4(3)	N(32)	1.1488(5)	−0.3640(5)	1.1768(5)	4.7(4)
O(22)	1.1728(4)	−0.3995(3)	1.2278(4)	5.2(3)	N(101)	1.5146(4)	−0.2259(3)	1.4339(2)	1.7(2)
O(23)	1.1395(5)	−0.3935(4)	1.1262(4)	8.0(4)	N(201)	1.2264(4)	−0.0841(3)	1.4334(2)	1.6(2)
O(31)	1.4150(3)	−0.0213(2)	1.3435(2)	2.4(2)	C(101)	1.3910(5)	−0.2521(4)	1.3005(3)	1.8(3)
O(101)	1.3906(3)	−0.1827(3)	1.2941(2)	2.3(2)	C(107)	1.4789(5)	−0.2960(3)	1.2937(3)	1.8(3)
O(102)	1.3231(3)	−0.2890(3)	1.3099(2)	2.9(2)	C(201)	1.1452(5)	−0.1014(4)	1.2884(3)	1.9(3)
O(201)	1.2152(3)	−0.0641(2)	1.2842(2)	2.2(2)	C(207)	1.0548(5)	−0.0597(4)	1.2936(3)	1.8(3)
O(202)	1.1397(4)	−0.1710(3)	1.2856(3)	3.5(2)					
				$[Mn_2(\mu\text{-}O)(XDK)(4,4'\text{-}Me_2bpy)_2(NO_3)_2]$·2.5$CH_3OH$ (**6**·2.5CH_3OH)					
Mn(1)	0.41062(4)	0.0570(1)	0.00081(9)	2.01(8)	N(11)	0.4409(2)	−0.0324(7)	0.0510(4)	2.4(5)
Mn(2)	0.33791(4)	0.0245(1)	0.03821(8)	2.00(8)	N(12)	0.4515(2)	0.1425(7)	0.0011(4)	2.2(5)
O(1)	0.3767(2)	−0.0219(6)	0.0158(3)	2.0(4)	N(21)	0.3150(2)	−0.0882(7)	−0.0101(5)	2.9(6)
O(11)	0.4309(2)	−0.0174(8)	−0.0806(5)	4.4(6)	N(22)	0.2907(2)	0.0620(7)	0.0520(4)	2.3(5)
O(12)	0.4048(3)	−0.154(1)	−0.0839(8)	12(1)	N(31)	0.4230(3)	−0.097(1)	−0.1068(7)	4.1(8)
O(13)	0.4359(3)	−0.119(1)	−0.1538(6)	8.5(9)	N(32)	0.3375(4)	−0.158(1)	0.1306(7)	5(1)
O(21)	0.3244(2)	−0.0795(8)	0.1168(4)	4.3(6)	N(101)	0.3667(2)	0.3766(7)	−0.0875(4)	1.8(5)
O(22)	0.3588(3)	−0.196(1)	0.1016(7)	8(1)	N(201)	0.3842(2)	0.3682(7)	0.1280(4)	1.9(5)
O(23)	0.3308(3)	−0.1985(9)	0.1806(5)	8.1(8)	C(101)[c]	0.3594(3)	0.1437(9)	−0.0713(5)	2.0(2)
O(101)	0.3886(2)	0.1451(6)	−0.0574(3)	2.3(4)	C(107)[c]	0.3513(3)	0.146(1)	−0.1380(5)	2.2(3)
O(102)	0.3364(2)	0.1331(5)	−0.0356(4)	2.7(4)	C(201)[c]	0.3809(3)	0.134(1)	0.1182(5)	2.0(2)
O(201)	0.4040(2)	0.1425(5)	0.0834(3)	1.9(4)	C(207)[c]	0.3863(3)	0.133(1)	0.1848(6)	2.5(3)
O(202)	0.3518(2)	0.1170(6)	0.1003(3)	2.3(4)					

[a] Estimated standard deviations are given in parentheses. [b] All atoms were refined with anisotropic thermal parameters given as the isotropic equivalent displacement parameter defined as $B_{eq} = (8\pi^2/3)(U_{11}(aa^*)^2 + U_{22}(bb^*)^2 + U_{33}(cc^*)^2 + 2U_{12}aa^*bb^*\cos\gamma + 2U_{13}aa^*cc^*\cos\beta + 2U_{23}bb^*cc^*\cos\alpha)$. [c] Refined isotropically.

N,N'-bis(2-pyridylmethyl)ethylenediamine) and $[Mn^{II}_2(\mu\text{-}OAc)_2(bpy)_4]^{2+}$ (4.5832(8) Å),[24] both of which have an unsupported bis(μ-carboxylato)dimetal core in which carboxylate groups bridge in a *syn–anti* bidentate manner. The carboxylate bridging mode in **1** is essentially *syn–syn*, despite considerable expansion of $Mn-O_{CO_2}-C_{CO_2}$ angles (vide infra). The distance is notably quite close to the glutamate-bridged metal–metal separation in the active site of xylose isomerases (4.9 Å), which require Mg^{2+}, Mn^{2+}, and Co^{2+} ions for activity. Recently, a dimagnesium complex isomorphous to **1**, $[Mg_2(XDK)(NO_3)(CH_3OH)_4(H_2O)_2](NO_3)$, was isolated and characterized.[31e] Its Mg···Mg distance of 4.783(2) Å is close to the Mn···Mn separation in compound **1**. This geometric similarity between carboxylate-bridged dinuclear Mn(II) and Mg(II) cores provides a structural rationale for the fact that Mg^{II}_2 units in the active centers of some redox-inactive enzymes can be replaced by Mn(II) ions without suppressing the catalytic activity.

As evident from Figure 1a, the two Mn atoms are located almost within the dicarboxylate plane. Our previous studies of Fe(III) complexes[31b] demonstrated that XDK can accommodate a significant out-of-plane distortion of the normal carboxylate bridging mode, with the $M-O_{CO_2}$ bonds located well out of the plane of the carboxylate group. Such a distortion was quantitated by the metal deviation (d) from the plane of carboxylate groups and the fold angle (ϕ) between the $[M_2(O_{CO_2})_2]$ plane and the carboxylate group. The average d and ϕ values in compound **1** are 0.28 Å and 10°, respectively, fairly small compared with those in $[Fe_2(\mu\text{-}O)(XDK)(CH_3OH)_5(H_2O)]^{2+}$ (d = 1.21 Å and ϕ = 37°). The d and ϕ values of **1** indicate little out-of-plane distortion of the bridging dicarboxylate, but some strain is apparent in the bond angles at the carboxylate oxygen atoms, the average $Mn-O_{CO_2}-C_{CO_2}$ being 155.5° (range 150.2(2)–160.8(2)°). The average $Mn-O_{CO_2}$ bond length of 2.087 Å (range 2.043(2)-2.116(2) Å) is normal for dinuclear Mn(II) complexes, suggesting that the $Mn-O_{CO_2}$ bonds are not weakened despite the distorted bond angles. The Mn(1) atom has pseudo-octahedral geometry and is coordinated by a bidentate nitrate anion, methanol, and water molecules in addition to the two carboxylate oxygen atoms of XDK. The Mn(2) atoms are similarly coordinated by three methanol and water molecules and by the two carboxylate oxygen atoms of XDK. The two water molecules are located in axial positions with respect to the Mn_2–dicarboxylate plane and are hydrogen bonded to both imino oxygen atoms of the XDK ligand framework (O(4)···O(104) = 2.806(3) Å, O(4)···O(204) = 2.777(3) Å, O(6)···O(103) = 2.782(3) Å, O(6)···O(203) =

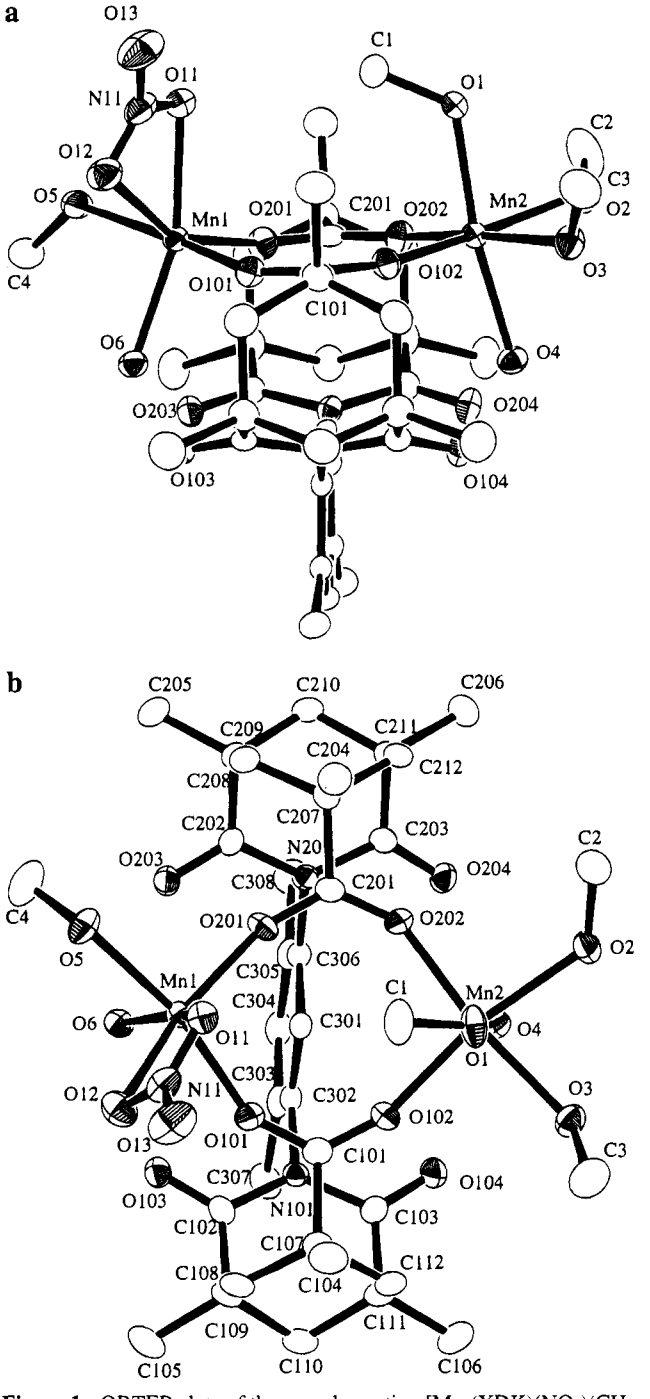

Figure 1. ORTEP plots of the complex cation $[Mn_2(XDK)(NO_3)(CH_3OH)_4(H_2O)_2]^+$ (cation of **1**) viewed (a) along and (b) perpendicular to the dicarboxylate plane. Thermal ellipsoids are drawn at the 40% probability level, and hydrogen atoms are omitted for clarity.

Table 3. Selected Bond Distances (Å) and Angles (deg) for $[Mn(XDK)(NO_3)(CH_3OH)_4(H_2O)_2](NO_3)$ (**1**)[a]

Bond Distances			
Mn(1)–O(5)	2.200(2)	Mn(1)–O(6)	2.181(2)
Mn(1)–O(11)	2.260(2)	Mn(1)–O(12)	2.345(2)
Mn(1)–O(101)	2.089(2)	Mn(1)–O(201)	2.043(2)
Mn(2)–O(1)	2.180(2)	Mn(2)–O(2)	2.213(2)
Mn(2)–O(3)	2.217(2)	Mn(2)–O(4)	2.180(2)
Mn(2)–O(102)	2.099(2)	Mn(2)–O(202)	2.116(2)
O(1)–C(1)	1.419(4)	O(2)–C(2)	1.396(5)
O(3)–C(3)	1.407(4)	O(5)–C(4)	1.418(4)
O(11)–N(11)	1.289(4)	O(12)–N(11)	1.247(4)
O(13)–N(11)	1.218(4)		
Bond Angles			
O(5)–Mn(1)–O(6)	87.87(8)	O(5)–Mn(1)–O(11)	83.20(8)
O(5)–Mn(1)–O(12)	89.70(9)	O(5)–Mn(1)–O(101)	167.88(9)
O(5)–Mn(1)–O(201)	93.10(9)	O(6)–Mn(1)–O(11)	162.65(8)
O(6)–Mn(1)–O(12)	109.48(8)	O(6)–Mn(1)–O(101)	89.77(8)
O(6)–Mn(1)–O(201)	97.16(8)	O(11)–Mn(1)–O(12)	55.82(8)
O(11)–Mn(1)–O(101)	95.84(8)	O(11)–Mn(1)–O(201)	98.16(9)
O(12)–Mn(1)–O(101)	79.88(8)	O(12)–Mn(1)–O(201)	153.31(9)
O(101)–Mn(1)–O(201)	98.99(9)	O(1)–Mn(2)–O(2)	84.76(9)
O(1)–Mn(2)–O(3)	92.10(9)	O(1)–Mn(2)–O(4)	172.00(8)
O(1)–Mn(2)–O(102)	89.98(9)	O(1)–Mn(2)–O(202)	93.76(9)
O(2)–Mn(2)–O(3)	81.49(9)	O(2)–Mn(2)–O(4)	89.42(9)
O(2)–Mn(2)–O(102)	167.89(9)	O(2)–Mn(2)–O(202)	91.37(9)
O(3)–Mn(2)–O(4)	81.58(8)	O(3)–Mn(2)–O(102)	87.83(9)
O(3)–Mn(2)–O(202)	170.31(8)	O(4)–Mn(2)–O(102)	94.66(8)
O(4)–Mn(2)–O(202)	91.87(8)	O(102)–Mn(2)–O(202)	99.87(9)
Mn(2)–O(1)–C(1)	121.2(2)	Mn(2)–O(2)–C(2)	129.4(2)
Mn(2)–O(3)–C(3)	127.3(2)	Mn(1)–O(5)–C(4)	130.5(2)
Mn(1)–O(11)–N(11)	94.3(2)	Mn(1)–O(12)–N(11)	91.5(2)
Mn(1)–O(101)–C(101)	150.4(2)	Mn(2)–O(102)–C(101)	160.5(2)
Mn(1)–O(201)–C(201)	160.8(2)	Mn(2)–O(202)–C(201)	150.2(2)

[a] Estimated standard deviations are given in parentheses. See Figure 1 for atom labels.

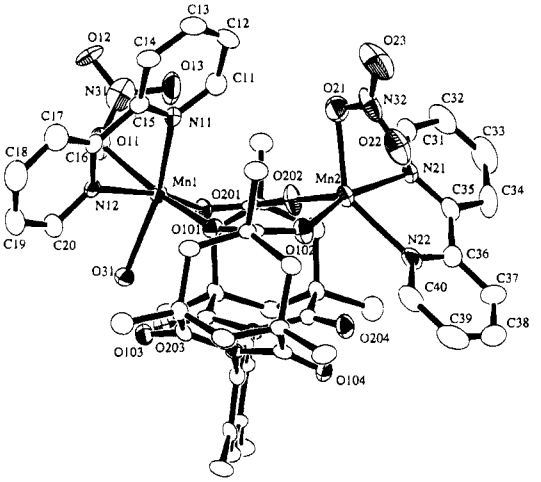

Figure 2. ORTEP drawing of $[Mn_2(XDK)(bpy)_2(NO_3)_2(H_2O)]$ (**2**). Thermal ellipsoids are given at the 40% probability level, and hydrogen atoms are omitted for clarity.

2.781(3) Å). The XDK ligand exhibits a sterically constrained structure; the Kemp's triacid imide moieties are nearly symmetrically disposed with respect to the xylyl ring, and the two carboxylate groups are almost coplanar, with a twist angle of only 6°. In the crystal packing diagram (not shown), a hydrogen bonding network may exist between the coordinated and uncoordinated nitrate anions and the coordinated methanol molecules: O(1)···O(21) $(-x + 2.0, -y + 1.0, -z + 2.0)$ = 2.793(3) Å, O(3)···O(22) (x, y, z) = 2.729(3) Å, and O(5)···O(11) $(-x + 3.0, -y, -z + 2)$ = 2.823(3) Å.

Structure of $[Mn_2(XDK)(bpy)_2(NO_3)_2(H_2O)]\cdot CH_2Cl_2$ ($2\cdot CH_2Cl_2$). A drawing of complex **2** with its atomic numbering scheme is given in Figure 2, and selected bond lengths and angles are listed in Table 4. The molecule consists of an asymmetrical dimanganese(II) core linked by two carboxylate groups of XDK. The Mn(II) atoms are 4.557(2) Å apart, 0.29 Å less than the corresponding distance in **1**. The out-of-plane distortion involving the dicarboxylate bridges is considerably greater in **2** than in **1**, with average d and ϕ values of 0.55 Å and 19°, respectively. The Mn(1) center is octahedrally coordinated by two carboxylate oxygen atoms of XDK, a bidentate bpy, a monodentate nitrate anion, and a water molecule. The water molecule is hydrogen bonded to the carbonyl oxygen atoms of imide moieties, O(31)···O(103) = 2.809(7) Å and O(31)···O(203) = 2.842(6) Å, interactions similar to those in **1**. The geometry at Mn(2) is best described as a distorted trigonal bipyramidal, comprising two carboxylate oxygen atoms of XDK, a bidentate bpy, and an oxygen atom

Table 4. Selected Bond Distances (Å) and Angles (deg) for $[Mn_2(XDK)(bpy)_2(NO_3)_2(H_2O)]\cdot CH_2Cl_2$ (**2**·CH_2Cl_2)[a]

Bond Distances			
Mn(1)–O(11)	2.246(5)	Mn(1)–O(31)	2.231(5)
Mn(1)–O(101)	2.146(5)	Mn(1)–O(201)	2.106(4)
Mn(1)–N(11)	2.242(6)	Mn(1)–N(12)	2.319(6)
Mn(2)–O(21)	2.202(6)	Mn(2)–O(102)	2.080(5)
Mn(2)–O(202)	2.063(5)	Mn(2)–N(21)	2.253(6)
Mn(2)–N(22)	2.228(7)	O(11)–N(31)	1.368(9)
O(12)–N(31)	1.247(8)	O(13)–N(31)	1.258(9)
O(21)–N(32)	1.273(9)	O(22)–N(32)	1.26(1)
O(23)–N(32)	1.222(9)		

Bond Angles			
O(11)–Mn(1)–O(31)	100.0(2)	O(11)–Mn(1)–O(101)	167.3(2)
O(11)–Mn(1)–O(201)	89.1(2)	O(11)–Mn(1)–N(11)	84.4(2)
O(31)–Mn(1)–O(101)	89.5(2)	O(31)–Mn(1)–O(201)	83.0(2)
O(31)–Mn(1)–N(11)	156.5(2)	O(101)–Mn(1)–O(201)	100.5(2)
O(101)–Mn(1)–N(11)	83.5(2)	O(201)–Mn(1)–N(11)	120.2(2)
O(201)–Mn(1)–N(12)	165.7(2)	O(101)–Mn(1)–N(12)	88.0(2)
O(31)–Mn(1)–N(12)	85.6(2)	N(11)–Mn(1)–N(12)	71.9(2)
O(11)–Mn(1)–N(12)	84.4(2)	O(21)–Mn(2)–O(102)	101.5(2)
O(21)–Mn(2)–O(202)	98.2(2)	O(21)–Mn(2)–N(21)	87.5(2)
O(21)–Mn(2)–N(22)	137.0(2)	O(102)–Mn(2)–O(202)	105.8(2)
O(102)–Mn(2)–N(21)	164.1(2)	O(102)–Mn(2)–N(22)	92.3(2)
O(202)–Mn(2)–N(21)	85.5(2)	O(202)–Mn(2)–N(22)	117.0(2)
N(21)–Mn(2)–N(22)	72.5(2)	Mn(1)–O(11)–N(31)	114.2(5)
Mn(2)–O(21)–N(32)	99.7(6)	Mn(1)–O(101)–C(101)	156.1(5)
Mn(2)–O(102)–C(101)	136.7(5)	Mn(1)–O(201)–C(201)	138.9(4)
Mn(2)–O(202)–C(201)	163.6(5)		

[a] Estimated standard deviations are given in parentheses. See Figure 2 for atom labels.

of a nitrate anion. The axial positions are occupied by the O(102) and N(21) atoms, and the dangling O(22) atom of the nitrate ion interacts weakly with Mn(2), Mn(2)–O(22) = 2.437(6) Å. The pentacoordinate geometry at Mn(2), which differs from the octahedral geometry found at Mn(1), may have arisen in order to avoid steric repulsion between two pyridyl units across the Mn···Mn vector.

Complex **2** and its analogs **3** and **4** could be good precursors of substrate-binding models for dimanganese enzymes, because the nitrate anions are substitutionally labile. They dissociate readily from the metal centers in methanol solution, affording a solvated dimanganese(II) complex cation, tentatively formulated as $[Mn_2(XDK)(bpy)_2(CH_3OH)_2(H_2O)]^{2+}$.

Synthesis and Structure of Dinuclear (μ-Oxo)dimanganese(III) Complexes with XDK. The dimanganese(II) complexes, $[Mn_2(XDK)L_2(NO_3)_2(H_2O)]$ (L = bpy (**2**), 4,4′-Me_2bpy (**3**)), formed in situ from the reaction between $[Mn_2(XDK)(NO_3)(CH_3OH)_4(H_2O)_2](NO_3)$ (**1**, 1 equiv) and L (2 equiv), are readily oxidized by an excess amount *tert*-butyl hydroperoxide (TBHP) in methanol to afford the (μ-oxo)dimanganese(III) complexes, $[Mn_2(\mu\text{-}O)(XDK)L_2(NO_3)_2]$ (L = bpy (**5**), 4,4′-Me_2bpy (**6**)), in good yields. Whereas $[^nBu_4N][MnO_4]$, $KMnO_4$, and H_2O_2 are usually employed as oxidizing reagents in preparing high-valent di- and polynuclear manganese complexes,[1] synthetic procedures using alkyl hydroperoxide are less well explored in Mn chemistry, although these reagents have been used as an oxygen source in manganese-catalyzed oxidations of alkanes and alkenes.[25,37] The formation of $[Mn^{III}Mn^{IV}(\mu\text{-}O)_2(bpy)_4]^{3+}$ and $[Mn^{IV}_2(\mu\text{-}O)_2(salpn)_2]$ was recently reported in reactions of $[Mn(bpy)_3]^{2+}$ and $[Mn^{III}_2(\mu\text{-}OCH_3)_2(salpn)_2]$, respectively, with TBHP.[37,38] The present reactions were very efficient, occurring without dioxygen evolution or the formation of side products, such as more highly oxidized and/or polynuclear manganese species. Complexes **5** and **6** could also be obtained by air oxidation of **2** and **3** in methanol, although the reaction proceeded slowly over several days and the yields were low.

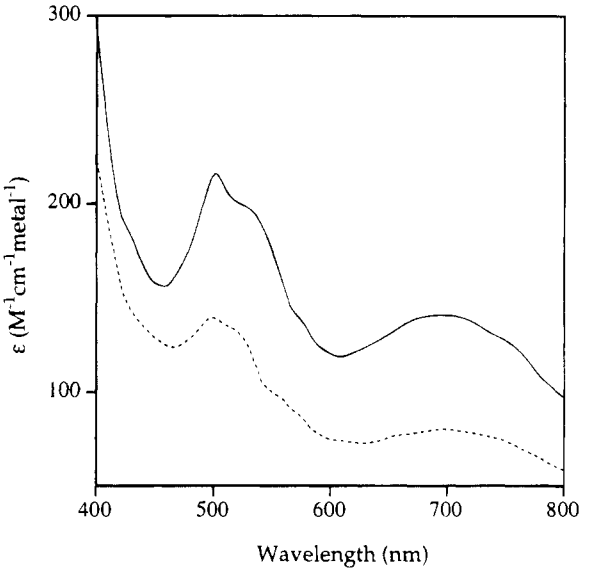

Figure 3. Electronic absorption spectra of **5** (···) and **6** (—) in methanol.

The IR spectra of **5** and **6** displayed characteristic XDK (~1700–1590 cm^{-1}), nitrate (~1300 cm^{-1}), and N-donor ligand absorptions. A medium and slightly broad band at 720–730 cm^{-1} was assigned to ν_{as}(Mn–O–Mn), by analogy to similar features in $[Mn_2(\mu\text{-}O)(\mu\text{-}OAc)_2(HB(pz)_3)_2]$ (**8**, 712 cm^{-1})[19] and $[Mn_2(\mu\text{-}O)(\mu\text{-}OAc)_2(Me_3tacn)_2](ClO_4)_2$ (**9**, 730 cm^{-1}).[20] The electronic spectra of **5** and **6** in methanol showed absorptions around 500 nm and a broad band centered at about 700 nm with modest molar extinction coefficients ranging from 80 to 218 M^{-1} cm^{-1} $metal^{-1}$ (Figure 3). The spectral patterns are essentially similar to those of **8** (486 nm (ϵ = 210 M^{-1} cm^{-1} $metal^{-1}$), 760 (58)), **9** (486 (337), 521 (323), 720 (56)), and the manganese catalase from *L. plantarum* (470 (135), 680 (36)),[1,3,19] indicating the presence of the Mn(III)–O–Mn(III) structure. The molar conductivity of **2** in methanol, 175 Ω^{-1} cm^2 mol^{-1}, corresponded to a 1:2 electrolyte, implying dissociation of nitrate anions from the dinuclear center. The cyclic voltammogram of **5** did not exhibit any redox activity within the potential limits in DMF. Complexes **5** and **6** are stable in methanol and DMF in the air but slowly decomposed to an uncharacterized brown precipitate following treatment with H_2O. In contrast, complexes **5** and **6** were readily transformed to the starting Mn(II) complexes **2** and **3** by treatment of H_2O_2 as evidenced by a color change from violet to pale yellow as well as by IR spectroscopy.

The structure of **6**·2.5CH_3OH was determined by X-ray crystallography. An ORTEP diagram with the atomic labeling scheme is presented in Figure 4, and selected bond lengths and angles are summarized in Table 5. The structure of **6** has a pseudo-C_2 symmetry axis passing through the O(1) atom and lying in the Mn–O–Mn plane. The two Mn(III) ions are linked by two carboxylate groups of XDK and an oxo ligand, with the terminal sites occupied by bidentate Me_2bpy and monodentate nitrate ion. The geometry of the dinuclear core is consistent with that of other $\{Mn_2(\mu\text{-}O)(\mu\text{-carboxylato})_2\}^{2+}$ complexes reported to date.[19–23] The Mn···Mn distance, 3.170(2) Å, is significantly shorter than that in $[Mn_2(XDK)(bpy)_2(NO_3)_2(H_2O)]$ (**2**, 4.557(2) Å), owing to the additional oxo bridge and the short

(37) For example: (a) Fish, R. H.; Fong, R. H.; Oberhausen, K. J.; Konings, M. S.; Vega, M. C.; Christou, G.; Vincent, J. B.; Buchanan, R. M. *New J. Chem.* **1992**, *16*, 727. (b) Ménage, S.; Collomb-Dunand-Sauthier, M.-N.; Lambeaux, C.; Fontecave, M. *J. Chem. Soc., Chem. Commun.* **1994**, 1885.
(38) Larson, E. J.; Pecoraro, V. L. *J. Am. Chem. Soc.* **1991**, *113*, 3810.

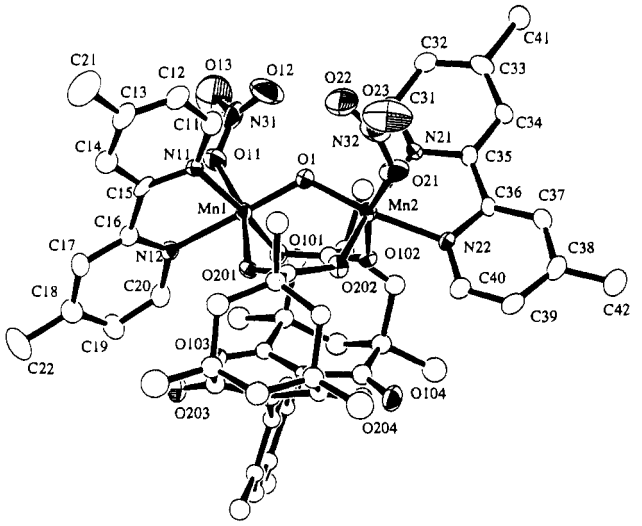

Figure 4. ORTEP diagram of $[Mn_2(\mu\text{-}O)(XDK)(4,4'\text{-}Me_2bpy)_2(NO_3)_2]$ (**6**). Thermal ellipsoids are drawn at the 40% probability level, and hydrogen atoms are omitted for clarity.

Table 5. Selected Bond Distances (Å) and Angles (deg) for $[Mn_2(\mu\text{-}O)(XDK)(4,4'\text{-}Me_2bpy)_2(NO_3)_2]\cdot 2.5CH_3OH$ ($\mathbf{6}\cdot 2.5CH_3OH$)[a]

Bond Distances			
Mn(1)–O(1)	1.781(7)	Mn(1)–O(11)	2.24(1)
Mn(1)–O(101)	1.968(8)	Mn(1)–O(201)	2.182(8)
Mn(1)–N(11)	2.06(1)	Mn(1)–N(12)	2.038(9)
Mn(2)–O(1)	1.799(7)	Mn(2)–O(21)	2.30(1)
Mn(2)–O(102)	2.185(8)	Mn(2)–O(202)	1.935(7)
Mn(2)–N(21)	2.07(1)	Mn(2)–N(22)	2.051(9)
O(11)–N(31)	1.24(1)	O(12)–N(31)	1.18(1)
O(13)–N(31)	1.22(1)	O(21)–N(32)	1.21(2)
O(22)–N(32)	1.21(2)	O(23)–N(32)	1.27(2)

Bond Angles			
O(1)–Mn(1)–O(11)	101.5(3)	O(1)–Mn(1)–O(101)	95.6(3)
O(1)–Mn(1)–O(201)	92.2(3)	O(1)–Mn(1)–N(11)	92.9(4)
O(1)–Mn(1)–N(12)	168.6(4)	O(11)–Mn(1)–O(101)	83.7(3)
O(11)–Mn(1)–O(201)	164.7(3)	O(11)–Mn(1)–N(11)	88.1(4)
O(11)–Mn(1)–N(12)	85.8(4)	O(101)–Mn(1)–O(201)	101.7(3)
O(101)–Mn(1)–N(11)	169.2(4)	O(101)–Mn(1)–N(12)	93.9(3)
O(201)–Mn(1)–N(11)	84.6(3)	O(201)–Mn(1)–N(12)	79.6(3)
N(11)–Mn(1)–N(12)	78.5(4)	O(1)–Mn(2)–O(21)	103.5(3)
O(1)–Mn(2)–O(102)	92.0(3)	O(1)–Mn(2)–O(202)	98.3(3)
O(1)–Mn(2)–N(21)	91.6(4)	O(1)–Mn(2)–N(22)	170.1(4)
O(21)–Mn(2)–O(102)	163.9(3)	O(21)–Mn(2)–O(202)	83.9(3)
O(21)–Mn(2)–N(21)	82.2(4)	O(21)–Mn(2)–N(22)	78.0(4)
O(102)–Mn(2)–O(202)	98.4(3)	O(102)–Mn(2)–N(21)	93.1(4)
O(102)–Mn(2)–N(22)	85.9(3)	O(202)–Mn(2)–N(21)	164.5(4)
O(202)–Mn(2)–N(22)	91.6(4)	N(21)–Mn(2)–N(22)	78.9(4)
Mn(1)–O(1)–Mn(2)	124.6(4)	Mn(1)–O(11)–N(31)	130.6(9)
Mn(2)–O(21)–N(32)	126(1)	Mn(1)–O(101)–C(101)	127.3(8)
Mn(2)–O(102)–C(101)	122.1(7)	Mn(1)–O(201)–C(201)	125.9(7)
Mn(2)–O(202)–C(201)	127.7(7)		

[a] Estimated standard deviations are given in parentheses. See Figure 4 for atom labels.

$Mn-O_{oxo}$ bonds. The average $Mn-O_{oxo}$ bond length and the $Mn-O_{oxo}-Mn$ angle are 1.790 Å and 124.6(4)°, respectively. The two Me_2bpy ligands have an anti arrangement with respect to the Mn–O–Mn plane. Similar structures have already been reported for $[Mn_2(\mu\text{-}O)(\mu\text{-}OAc)_2(X)_2]$ (X = Cl, N_3) and $[Mn_2(\mu\text{-}O)(\mu\text{-}OAc)_2(H_2O)_2](X)_2$ (X = PF_6, ClO_4).[22,23] Each Mn atoms is coordinated by a $[N_2O_4]$ set of donor atoms derived from XDK, Me_2bpy, nitrate, and oxo ligands. The octahedral environment around each metal center is somewhat distorted, with average $O_{CO_2}-Mn-O_{CO_2}$ = 100.1°, N_t-Mn-N_c = 78.7°, and $O_{oxo}-Mn-N_t$ = 169.4°, where N_t and N_c indicate the nitrogen atoms in positions trans and cis to the oxo ligand, respectively. There is also Jahn–Teller elongation along the $O_{CO_2}-Mn-O_{NO_3}$ axis, as usually observed in high-spin d^4 Mn-

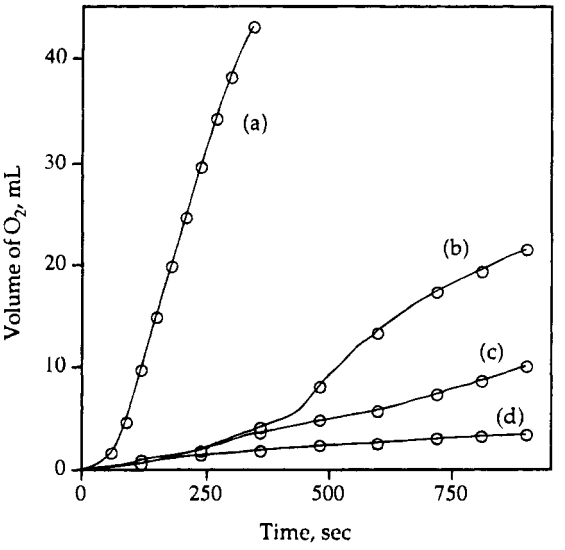

Figure 5. Time–course profiles of dioxygen evolution (mL) from the reaction of H_2O_2 (10 mmol) with (a) **1** (40 μmol), (b) **1** (40 μmol) and 4,4′-Me_2bpy (80 μmol), (c) **1** (40 μmol) and phen (80 μmol), and (d) **1** (40 μmol) and bpy (80 μmol), in 20 mL of methanol at 24 °C.

(III) complexes. The $Mn-O_{CO_2}$ bond lengths are divided into two groups; the O(101) and O(202) atoms have shorter bonds to the metal (average 1.952 Å; range 1.935(7)–1.968(8) Å), and the O(102) and O(201) atoms, longer ones (average 2.184 Å; range 2.182(8)–2.185(8) Å). The $Mn-N_c$ and $Mn-N_t$ bond lengths are almost identical within the experimental error, the average values being 2.065 and 2.045 Å, respectively. The dicarboxylate bridge of XDK demonstrates the typical out-of-plane distortion, first observed in (μ-oxo)diiron(III) complexes of XDK. The structural parameters, d = 1.24 Å and ϕ = 38°, are very similar to those of $[Fe_2(\mu\text{-}O)(XDK)(CH_3OH)_5(H_2O)]^{2+}$ (**10**, d = 1.21 Å, ϕ = 37), $[Fe_2(\mu\text{-}O)(XDK)(bpy)_2(NO_3)_2]$ (**11**, d = 1.21 Å, ϕ = 37°), and $[Fe_2(\mu\text{-}O)(XDK)(1\text{-}MeIm)_6]^{2+}$ (**12**, d = 1.20 Å, ϕ = 37°), which have recently been prepared as substitutionally labile models for non-heme iron proteins. In particular, compound **11** possesses a structural motif identical to that in **6** except for the arrangement of bpy ligands.[31b]

The present series of dimanganese complexes displays the ability of the dinucleating XDK ligand to accommodate a wide range of metal–metal separations (3.2–4.9 Å) in dimetallic complexes, suggesting its potential utility to mimic various types of biological centers involving dimanganese units.

Reaction of Dinuclear Mn(II) Complexes with Hydrogen Peroxide. Recent spectroscopic studies of manganese catalase and pseudocatalase have suggested a mechanism involving interconversion between the Mn^{II}_2 and Mn^{III}_2 oxidation states as the enzyme disproportionates hydrogen peroxide to H_2O and O_2.[1,3–5] This spectroscopic evidence has motivated inorganic chemists to prepare functional models that undergo similar redox chemistry, although efficient catalytic activity has already been observed in higher oxidation state couples, such as Mn(III)/Mn(IV).[28,39] The compounds $[Mn^{II}_2(L)(\mu\text{-}OAc)]^{2+}$ (**13**, HL = *N,N,N′,N′*-tetrakis(2-methylenebenzimidazolyl)-1,3-diaminopropan-2-ol)[6] and $Na_2[Mn^{II}_2(2\text{-}OHsalpn)_2]$ (**14a**) or $[Mn^{III}_2(2\text{-}OHsalpn)_2]$ (**14b**) (2-OHsalpn = 1,3-bis(salicylidenimino)-2-propanol)[7] have been reported, more recently, as plausible functional models for the natural catalase systems, and their catalytic mechanism was shown to proceed through a Mn^{II}_2/

(39) (a) Naruta, Y.; Maruyama, K. *J. Am. Chem. Soc.* **1991**, *113*, 3595. (b) Larson, E. J.; Pecoraro, V. L. *J. Am. Chem. Soc.* **1991**, *113*, 7809. (c) Stibrany, R. T.; Gorun, S. M. *Angew. Chem., Int. Ed. Engl.* **1990**, *29*, 1156.

Scheme 1

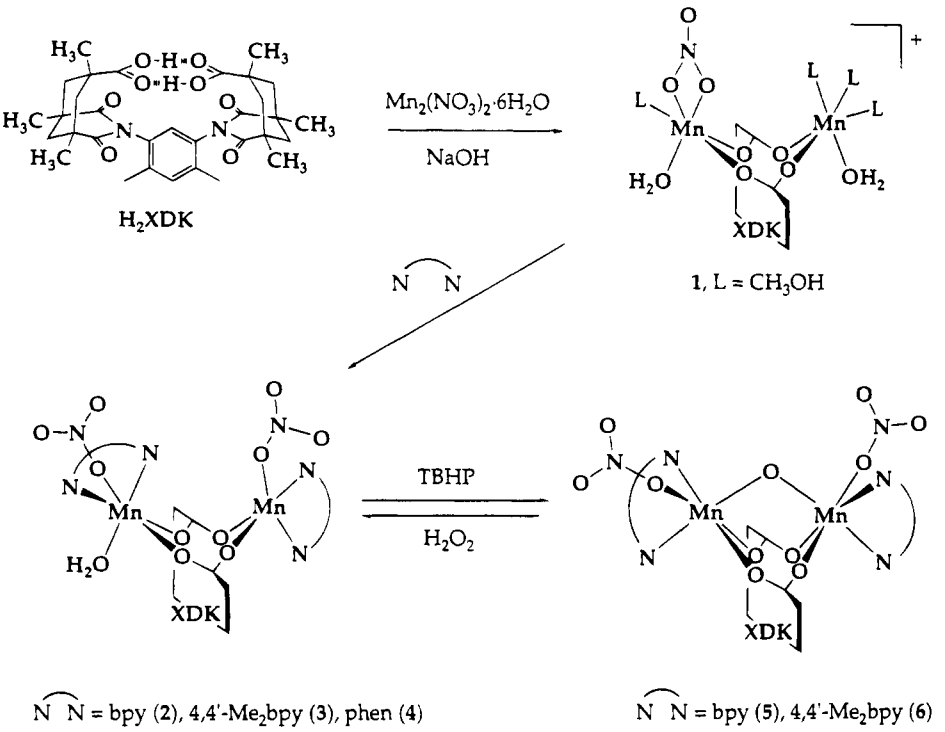

Mn^{III}_2 redox cycle. Dinuclear Mn(II) complexes with Schiff-base macrocyclic ligands (L), $[Mn^{II}_2L(\mu\text{-}X)](ClO_4)$ (X = halide, pseudohalide, and carboxylate) (**15**), have also been demonstrated to promote a catalase reaction, but a detailed redox mechanism was not clearly delineated.[40] It was therefore of interest to us, in this context, to investigate the ability of the present dinuclear Mn(II) XDK complexes to display catalase activity.

Accordingly, compounds **1**–**4** (~40 μmol) were treated with an excess of H_2O_2 (~10 mmol), and the evolution of dioxygen was monitored volumetrically (Figure 5). In the reaction of **1** there was a brief induction period, followed by vigorous evolution of dioxygen. The maximum evolution rate (v_{max}) was 0.18 mol of O_2/mol of **1**/s. The presence of a lag period suggested that **1** was not the true catalyst. A similar induction period was reported in the H_2O_2 disproportionation reaction by complexes **13** and **15**. The initial colorless reaction solution of **1** turned brown during the course of the reaction, and a heterogeneous mixture formed. This brown reaction mixture was confirmed to have activity even after consuming a 1000-fold excess of H_2O_2 without another induction period. From the mixture were isolated the mononuclear Mn(II) complex, $[Mn(HXDK)_2(H_2O)_2]$ (**7**), and MnO_2. The latter showed the catalytic activity, whereas the former did not, strongly suggesting that MnO_2 is the true catalyst in this system. The oxidation of Mn(II) ions seems to have been accelerated by the dinuclear Mn assembly in **1**, since $Mn(NO_3)_2{\cdot}6H_2O$ displayed no catalase activity under the same reaction condition. Complex **7** could be independently prepared by reaction of $Mn(NO_3)_2{\cdot}6H_2O$ (1 equiv) with H_2XDK (2 equiv) and NaOH (2 equiv) and is inferred to have an octahedral mononuclear structure, analogous to that of the structurally characterized complex $[Mg(HXDK)_2(H_2O)_2]$.[41]

In contrast to the reaction of **1**, O_2 evolution was considerably suppressed by N-donor bidentate ligands in **2**–**4**, with v_{max} = 2.2×10^{-2} to 7.8×10^{-2} s^{-1}. Comparison of activities showed **3** to be the best, after a long lag period. The pale yellow color of **3** in solution remained throughout the reaction, and complex **3** could be recovered from the homogeneous reaction mixture. At present, we cannot propose any mechanistic details. The possibility cannot be ruled out that a trace amount of MnO_2, derived from decomposition of **2**–**4**, promotes the apparent disproportionation of H_2O_2, since we observed an induction period and low activity. The N-donor bidentate ligands may protect the dinuclear Mn(II) core from oxidative decomposition by hydrogen peroxide.

Conclusions

The cleft-shaped dicarboxylate ligand XDK provides an efficient platform for synthesizing a series of the bis(μ-carboxylato)dimanganese(II) complexes, $[Mn_2(XDK)(NO_3)(CH_3OH)_4(H_2O)_2](NO_3)$ (**1**) and $[Mn_2(XDK)(NO_3)_2L_2(H_2O)]$ (L = bpy (**2**), 4,4'-Me_2bpy (**3**), phen (**4**)) (Scheme 1). Compound **1** undergoes oxidative decomposition by both *tert*-butyl hydroperoxide (TBHP) and hydrogen peroxide. The N-donor bidentate ligands in **2**–**4** significantly alter the reactivity of the Mn^{II}_2 center. Reactions of **2** and **3** with TBHP resulted exclusively in transformation to (μ-oxo)bis(μ-carboxylato)dimanganese(III) complexes, although **2**–**4** were resistant to oxidation by hydrogen peroxide. Finally, X-ray crystallographic studies have demonstrated that the dinucleating carboxylates of XDK can accommodate a wide range of nonbonded Mn···Mn distances, as the complexes interconvert between Mn^{II}_2 (~4.6 Å) and Mn^{III}_2 (~3.2 Å) cores.

Acknowledgment. This work was supported by a grant from the National Science Foundation. T.T. is grateful to the Shigaku Shinko Zaidan for an International Research Fellowship.

Supporting Information Available: Tables of crystallographic and experimental data, complete atomic positional and thermal parameters, and bond distances and angles for **1**, **2**·CH_2Cl_2, and **6**·2.5CH_3OH (39 pages). Ordering information is given on any current masthead page.

IC950199U

(40) Nagata, T.; Ikawa, Y.; Maruyama, K. *J. Chem. Soc., Chem. Commun.* **1994**, 471.

(41) Yun, J. W.; Lippard, S. J. Unpublished results.